

Site dependence of the Kondo scale in $\text{CePd}_{1-x}\text{Rh}_x$ due to Pd-Rh disorder

U. Stockert,^{1,*} S. Hartmann,¹ M. Deppe,¹ N. Caroca-Canales,¹ J. G. Sereni,² C. Geibel,¹ and F. Steglich¹

¹MPI for Chemical Physics of Solids, D-01187 Dresden, Germany

²Laboratorio de Bajas Temperaturas, Centro Atómico Bariloche (CNEA), S. C. de Bariloche 8400, Argentina

(Received 2 June 2015; published 10 August 2015)

We present measurements of the thermopower $S(T)$ on $\text{CePd}_{1-x}\text{Rh}_x$ between 2 K and 300 K. For low Rh content, the system behaves as a ferromagnetic Kondo system with a Curie temperature T_C of about 6 K, a Kondo scale smaller than T_C , and an overall crystal electric field splitting of 210 K. As the Rh content increases T_C is suppressed, while the average Kondo scale gets larger. Simultaneously, the presence of different Ce environments leads to a broad distribution of local Kondo scales ranging from very small values to above 50 K. As a consequence, large thermopower values are observed over an extended temperature range. Close to the critical concentration we find power-law dependencies of S/T vs T down to 2 K. For a Rh content of $x = 0.95$ we may show explicitly that the thermopower contains contributions from Ce sites with different local energy scales.

DOI: 10.1103/PhysRevB.92.054415

PACS number(s): 71.27.+a, 72.15.Jf, 75.20.Hr

I. INTRODUCTION

Heavy-fermion (HF) systems have been investigated intensively during the past decades due to their various exotic properties, such as unconventional superconductivity, quantum criticality, and non-Fermi-liquid behavior [1–3]. Chemical substitution is frequently used to tune the properties of HF systems, e.g., to suppress a magnetic ordering temperature to zero to reach a quantum critical point (QCP). In doing so it is usually assumed that the substitution changes the properties of the system on the whole, but not locally at each substituted site. In fact, isoelectronic substitution of a nonmagnetic element is often equivalent to chemical pressure. This means that the volume effect is comparable to the one in pressure experiments, and that other effects are negligible, at least for the problem under study. The disorder introduced by the substitution is relevant for the transport properties only in terms of larger impurity scattering leading to, e.g., an increase of the residual resistivity ρ_0 . The situation is more difficult in case of nonisoelectronic substitution. It can induce significant changes in the band structure and, consequently, the Fermi surface and the density of states (DOS). However, it is still usually assumed that the system behaves homogeneously, e.g., with respect to energy scales. In this paper we investigate $\text{CePd}_{1-x}\text{Rh}_x$, a system for which this assumption does not hold.

CePd is a ferromagnet with a Curie temperature $T_C = 6.6$ K [4,5]. Upon substitution of Pd by Rh T_C is suppressed continuously in $\text{CePd}_{1-x}\text{Rh}_x$ till it disappears at a critical concentration of about $x_{\text{cr}} = 0.87$ [6–8]. Pure CeRh exhibits the typical behavior of an intermediate valent (IV) system with a valence 3.17 ± 0.01 determined from L_{III} absorption measurements [5,7]. The evolution of $\text{CePd}_{1-x}\text{Rh}_x$ with increasing x is the result of both a decreasing unit-cell volume V_{uc} and, more important, a changing electronic environment of the Ce sites. These effects lead to an increasing hybridization of the Ce $4f$ states and a strong enhancement of the average Kondo temperature $T_K^{\text{av}} = T_K$ with larger x .

Three characteristic concentrations have been determined for $\text{CePd}_{1-x}\text{Rh}_x$ [7]: At $x = 0.65$ the phase boundary to ferromagnetic order $T_C(x)$ has an inflection point, leading to

a tail in the phase diagram. At slightly larger $x = 0.75$, a deviation from Vegard's law is observed, i.e., a change in the slope of $V_{\text{uc}}(x)$. This is due to a valence instability as confirmed by the rapid decrease of the $4f$ occupancy and the strongly increasing average Kondo scale at higher x . A third characteristic concentration is the critical one, $x_{\text{cr}} = 0.87$, at which the Curie temperature is suppressed to zero. It has been speculated that the occurrence of these three effects in such a narrow x range has the same origin, namely the random distribution of Kondo and magnetic interactions due to Pd/Rh disorder.

The relevance of disorder especially for $x \geq 0.65$ is confirmed by various experimental probes. Specific heat measurements on single and polycrystals revealed sharp anomalies at the ferromagnetic transitions indicating a homogeneous behavior of the system with respect to T_C up to $x = 0.6$, despite the disorder introduced by the substitution [6,9]. On the other hand, for $x \geq 0.65$, the transition is significantly broadened [7]. A wide distribution of local Kondo temperatures T_K^{loc} from 2 K to above 50 K is suggested by specific heat and susceptibility measurements for $x \geq 0.8$ and has been attributed to the presence of different Ce environments [8,10]. This finding is also in line with neutron scattering and μSR experiments on a sample with $x = 0.85$ [11]. Moreover, the presence of unscreened magnetic moments down to temperatures well below T_K^{av} is held responsible for the irreversibility of the magnetic susceptibility for $x \geq 0.65$ due to the formation of magnetic clusters [8].

The thermopower is very sensitive to Kondo scattering [12] in highly diluted [13] as well as concentrated Kondo systems [14]. For Ce-based Kondo systems large positive values are usually observed around T_K [15–17]. Contrary to specific heat or resistivity, the magnitude of the signal does not scale with the amount of magnetic ions, i.e., the thermopower of a dilute system may be similarly large as the one of a Kondo lattice as seen, for instance, in $\text{Ce}_x\text{La}_{1-x}\text{Al}_3$ [18], $\text{Ce}_x\text{La}_{1-x}\text{Pd}_2\text{Si}_2$ [19], and $\text{Ce}_x\text{La}_{1-x}\text{Cu}_{2.05}\text{Si}_2$ [20]. This is due to the fact that the thermopower is not proportional to the DOS itself but rather to its energy dependence [21]. It makes the thermopower an ideal tool to study the site dependence of the Kondo scale in $\text{CePd}_{1-x}\text{Rh}_x$. In a simplified picture, we expect a positive thermopower contribution for each type of Ce environment with a maximum around the respective T_K^{loc} . Therefore, a broad distribution of local Kondo scales as suggested for

*ulrike.stockert@cpfs.mpg.de

CePd_{1-x}Rh_x should lead to large thermopower values over an extended temperature region and down to low T .

II. EXPERIMENTAL DETAILS

We investigated polycrystalline samples of CePd_{1-x}Rh_x with $x \geq 0.6$. In addition we present data on the polycrystalline reference LaRh and on three single crystals ($x = 0.2, 0.4, 0.7$). The polycrystals were synthesized by arc melting of stoichiometric amounts of the pure elements [7]. The single crystals were grown using the Bridgeman technique [9,22]. Samples from these batches have been characterized previously by different crystallographic and thermodynamic probes [7–10,22]. From a crystallographic point of view, the system is homogeneous without cluster formation.

Simultaneous measurements of the thermopower and the electrical resistivity were performed using the thermal transport option of a PPMS. Resistivity data look similar to those presented in Ref. [7] and are used only for the calculation of thermopower contributions. For the single crystals, the heat current q was applied perpendicular to the b axis. Due to the small size and platelike shape of the crystals with b as the short dimension, measurements could be performed only for selected orientations. However, we expect a rather isotropic thermopower at least for $x \geq 0.7$ since the magnetic anisotropy is weak [22]. Measurements for $x = 0.4$ confirmed a very weak direction dependence for $q \parallel a$ and $q \parallel c$ also at this concentration. Moreover, the systematic change of the thermopower with substitution, especially for the three compositions $x = 0.6, 0.7$, and 0.75 , is in line with a weak anisotropy of S . In the following we will therefore not distinguish between measurements on single crystals and polycrystals, except for our discussion of the ferromagnetic ordering transition.

III. RESULTS

A. Thermopower of CeRh

The thermopower of the IV system CeRh ($x = 1$) is plotted in Fig. 1 in the temperature range from 5–320 K. The inset shows the thermopower of the nonmagnetic reference compound LaRh. CeRh exhibits an overall positive thermopower with a large maximum around 220 K as frequently observed for Ce-based IV systems. By contrast, an almost linear negative thermopower $S \propto T$ is found for LaRh. This latter behavior is typical for simple metals with electronlike charge carriers in the absence of a significant phonon drag contribution. A linear fit over the whole temperature range yields a very good description of the data with a slope of $-0.05 \mu\text{V}/\text{K}$. Since no phonon drag contribution is observed in LaRh, we expect that it is also negligible in the whole substitution series CePd_{1-x}Rh_x.

The thermopower of IV systems is frequently discussed within a configuration-crossover model proposed by Hirst [23] and first applied to thermopower data by Gottwick *et al.* [24]. The model assumes a DOS of Lorentzian shape with a peak at an energy $(\epsilon_0 - \epsilon_F)$ with respect to the Fermi level ϵ_F and a width W . The temperature dependence of the magnetic contribution to the thermopower S_{mag} is then given by:

$$S_{\text{mag}}(T) = \frac{AT}{T^2 + B^2} \quad (1)$$

with the parameters $A = 2(\epsilon_0 - \epsilon_F)/|e|$ and $B^2 = 3[(\epsilon_0 - \epsilon_F)^2 + (W/2)^2]/(\pi k_B)^2$. A and B are directly related to the position $T_{\text{max}} = B$ and value $S_{\text{max}} = A/2B$ of the maximum in $S_{\text{mag}}(T)$. Alternatively, the data may be fitted to Eq. (1). A determination of S_{mag} is more complicated than in the case of, e.g., resistivity data. This is due to the fact that contributions from different scattering mechanisms add weighted by the corresponding resistivities according to the Gorter-Nordheim relation:

$$S\rho = S_{\text{mag}}\rho_{\text{mag}} + S_{\text{ref}}\rho_{\text{ref}}. \quad (2)$$

S_{ref} and ρ_{ref} are usually taken as the thermopower and electrical resistivity of a nonmagnetic reference compound. For the calculation of S_{mag} we use the electrical resistivities measured simultaneously with S (not shown), which look similar to those published in Ref. [7]. The result of such an analysis is shown in Fig. 1. The magnetic contribution S_{mag} is larger than the measured thermopower due to the negative contribution to S from normal (light) charge carriers, but the overall shape is not changed. From a fit of S_{mag} above 100 K to Eq. (2) we obtain $A = 27100 \mu\text{V}$ and $B^2 = 51100 \text{K}^2$ corresponding to $W = 65.2 \text{meV}$ and $(\epsilon_0 - \epsilon_F) = 13.6 \text{meV}$. The calculated thermopower curve is shown as a dashed line in Fig. 1. It is in good agreement with the measured thermopower around the maximum. At lower temperatures, the measured thermopower is lower than the calculated one. Similar deviations have been observed in other IV systems and may be due to additional scattering mechanisms [25] or due to the simplicity of the DOS used in the model.

As expected for a Ce system, $(\epsilon_0 - \epsilon_F)$ is positive, i.e., the resonance is lying above the Fermi level. The parameters $(\epsilon_0 - \epsilon_F)$ and W can be used for a determination of the valence, e.g., from the implicit formula Eq. (17) of Ref. [23]:

$$\frac{2(\epsilon_F - \epsilon_0)}{W} = \tan\left(\frac{\pi}{2} \frac{Y^{(-)} - Y^{(+)}}{Y^{(-)} + Y^{(+)}}\right), \quad (3)$$

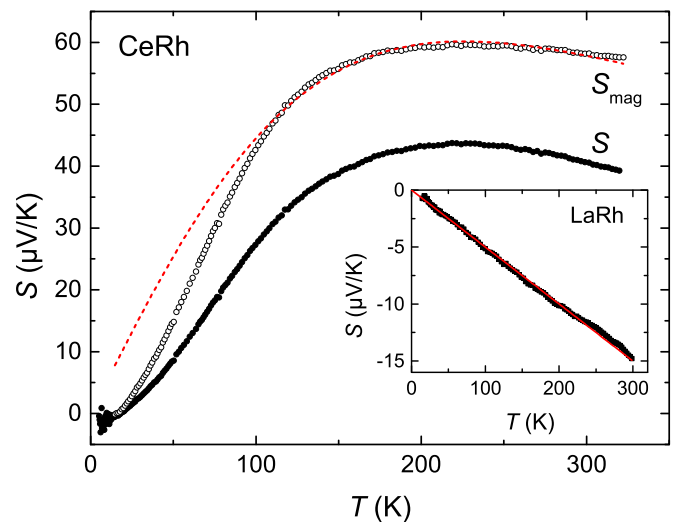


FIG. 1. (Color online) Main plot: Thermopower $S(T)$ of CeRh and its magnetic contribution S_{mag} . The line is a fit to the configuration-crossover model. Inset: Thermopower of the nonmagnetic reference LaRh. The line is a linear fit $S \propto T$.

where $Y^{(-)} = (1 - z)Q^{(-)}$ and $Y^{(+)} = zQ^{(+)}$. The quantities $Q^{(\pm)}$ are calculated in Ref. [23] for different ground states. Equation (3) allows a numerical determination of the $4f$ population parameter z , which is directly related to the valence $\nu_{\text{Ce}} = 3 + z$ for Ce systems. In our case we obtain $\nu_{\text{Ce}} = 3.15$ using $Q^{(-)} = 1$ and $Q^{(+)} = 6$ for the LSJ ground state of Ce. This value is in reasonable agreement with the one determined in L_{III} absorption measurements of 3.17 ± 0.01 [5,7]. We would also like to mention that a very similar valence of $\nu_{\text{Ce}} = 3.19$ is obtained, if we use directly S instead of S_{mag} for fitting Eq. (1) as sometimes done [25,26]. Therefore, we believe that uncertainties of the geometry factors of the electrical resistivities as well as the limited validity of Eq. (2) for dense Kondo systems (see below) are of minor relevance for the estimation of the valence.

B. Thermopower of CePd_{1-x}Rh_x

The thermopower of CePd_{1-x}Rh_x is plotted in Fig. 2. The low-temperature range of the samples with ferromagnetic ordering above 2 K is shown again in Fig. 3 on a larger scale. We describe our data starting from the highest Rh content $x = 1$ towards lower x . As mentioned above, pure CeRh

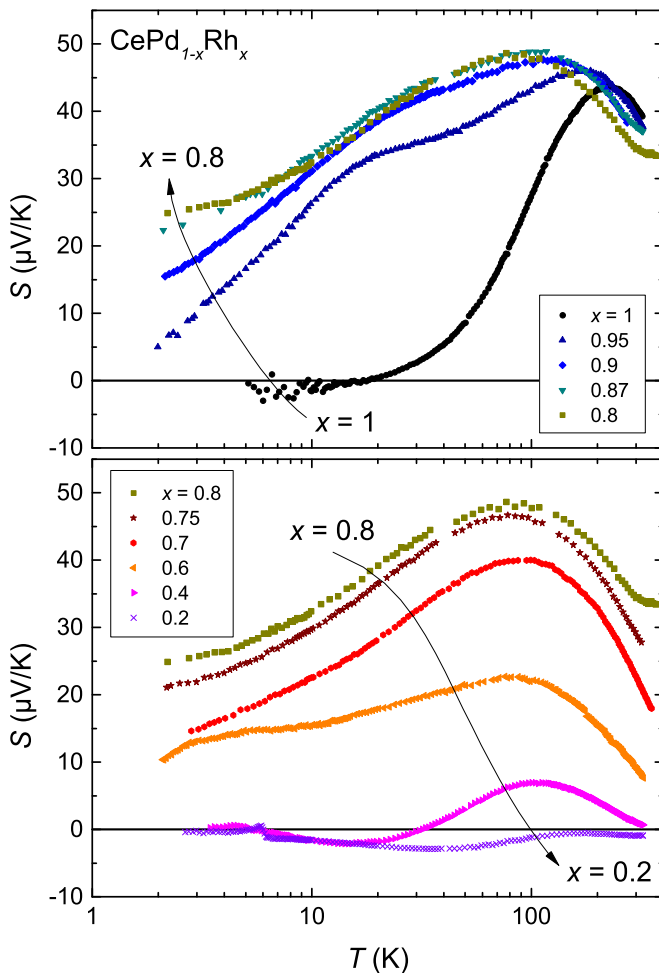


FIG. 2. (Color online) Thermopower of CePd_{1-x}Rh_x for $x \geq 0.8$ (top) and $x \leq 0.8$ (bottom).

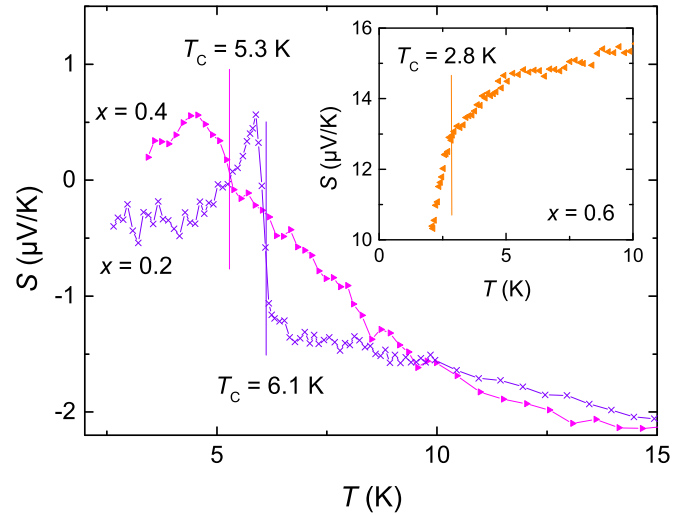


FIG. 3. (Color online) Low-temperature thermopower of the ferromagnetic samples. The main plot shows the data for single crystals with $x = 0.2, 0.4$. Data on a polycrystal with $x = 0.6$ are plotted in the inset. The Curie temperatures marked by vertical lines are taken from Refs. [7,9] and determined from specific heat measurements on crystals from the same batches.

($x = 1$) exhibits the typical behavior of an IV system with a single large maximum around 220 K. Substitution of Rh by Pd has four major effects on the thermopower: (i) With the Rh content x decreasing from 1–0.8 the large maximum at high temperatures is shifted towards lower T . (ii) Simultaneously, a strong enhancement of the low-temperature thermopower is observed for $0.95 \geq x \geq 0.7$. This is accompanied by the formation of a shoulder around 20 K for $0.95 \geq x \geq 0.87$, which is, however, absent for $0.8 \geq x \geq 0.7$. (iii) A second, very weak maximum or plateau appears again for the sample with $x = 0.6$ below 10 K. (iv) Kinks are observed in the thermopower at the transitions to the ferromagnetic state.

In the following we discuss these observations upon increasing x , i.e., starting from the Kondo behavior. We begin with the last observation: Clear kinks at T_C followed by maxima are seen in the single crystal data ($x = 0.2, 0.4$). By contrast, the polycrystalline sample with $x = 0.6$ exhibits only a weak change in slope below T_C . This is reminiscent of specific heat measurements on samples from the same batches, which show somewhat sharper transitions for the single crystals [9] than for a polycrystal with $x = 0.6$ [7]. The differences in $S(T)$ are therefore probably at least to some extent due to the different sample quality. In general, signatures of T_C in $S(T)$ are rather diverse for Kondo lattices, ranging from no clear feature (e.g., in CeIr₂B₂ [27]) over a tiny inflection (Ce₃RhSi₃ [28]) to kinks followed by a strong decrease or increase (CeAgSb₂ [29], CeFePO [30]). In the absence of any theoretical model for the thermopower of ferromagnetic Kondo systems we may only speculate that the kinks in $S(T)$ are due to changes in the DOS or to reduced spin disorder scattering below T_C . The maximum seen below T_C for $x \leq 0.4$ might be due to a magnon drag contribution. In fact, a considerable magnon contribution to the specific heat and electrical resistivity has been detected in

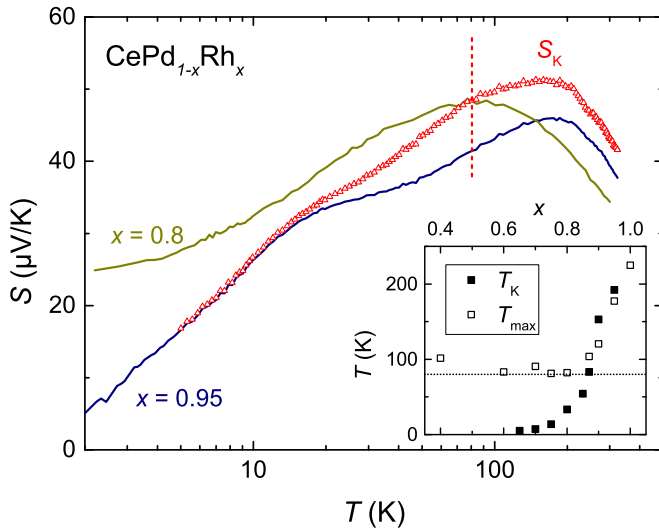


FIG. 4. (Color online) Main plot: The Kondo contribution S_K to the thermopower for $x = 0.95$ (for definition and determination see text). A shoulder appears at the position of the maximum in $S(T)$ for $x = 0.8$ marked by a vertical line, which is not seen in the thermopower of $x = 0.95$. Inset: Position of the maximum T_{\max} in $S(T)$ in comparison to the Kondo temperature T_K estimated as half the Weiss temperature (taken from Ref. [7]). For $x < 0.85$, T_{\max} is almost constant, while it shifts with the Kondo temperature for higher x . The horizontal line marks the same value as the vertical line in the main plot (80 K).

single crystals with $x = 0.2, 0.4$, but not for a single crystal with $x = 0.6$ [9].

Next we turn to the first and third observation, which can be explained by the evolution of $\text{CePd}_{1-x}\text{Rh}_x$ from a ferromagnetic Kondo system to an IV compound with increasing x . At low x the Kondo scale T_K of $\text{CePd}_{1-x}\text{Rh}_x$ is much smaller than the crystal electric field (CEF) splitting T_{CEF} . Therefore, two maxima are expected in $S(T)$: one around T_K due to Kondo scattering on the ground-state doublet [15–17], and another one around $(0.3\text{--}0.6) T_{\text{CEF}}$ due to scattering on the full Ce^{3+} multiplet [15,31,32]. We ascribe the plateau seen below 10 K for $x = 0.6$ to Kondo scattering on the ground-state doublet. Most probably the ferromagnetic ordering with T_C of the same order as T_K prevents the occurrence of clear low- T maxima in the samples with $x \leq 0.4$. As T_K increases, the (presumed) two maxima merge into a single large one for $x \geq 0.7$ [33,34]. At even higher x the Kondo scale gets of the same order as the CEF splitting, and the system enters the IV regime characterized by a sixfold degenerate ground state. A large maximum around T_K is observed in $S(T)$ that shifts to higher T with increasing T_K . The inset of Fig. 4 illustrates this evolution. It shows the position T_{\max} of the high-temperature maximum in $S(T)$ together with the (average) Kondo temperature T_K estimated as half the Weiss temperature [7]. T_{\max} takes an almost constant value of about 80 K for $x \leq 0.8$ as indicated by the horizontal line and in agreement with the estimated overall CEF splitting of about $T_{\text{CEF}} = 210$ K [9]. At higher x it roughly follows T_K as expected in the IV state.

The picture presented so far is, however, unable to explain the second observation, namely the enhanced low-temperature thermopower for small and moderate Pd content ($0.7 \leq x \leq$

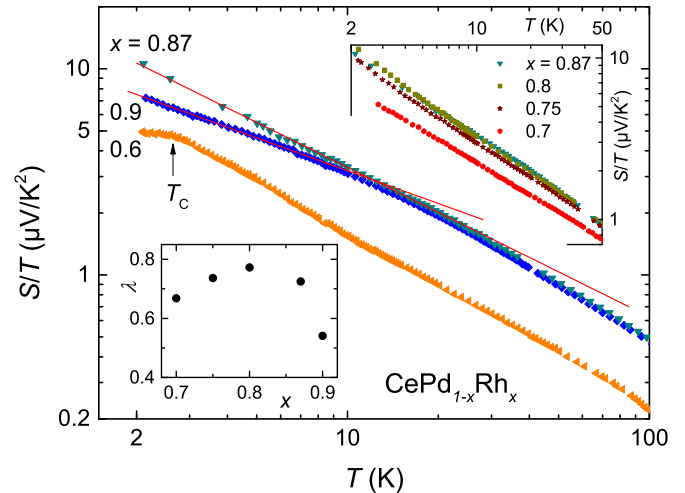


FIG. 5. (Color online) Thermopower divided by temperature. The sample with $x = 0.87$ exhibits a power-law dependence $S/T \propto T^{-\lambda}$ with an exponent of 0.72 below 30 K as indicated by a line in the main plot. Similar exponents λ are found for $0.7 \leq x \leq 0.87$ (insets). At lower and higher x clear deviations from a power law are observed, although a power law with smaller exponent can describe the data for $x = 0.9$ below 10 K (main plot).

0.95). The thermopower divided by temperature S/T increases strongly down to 2 K for $0.6 \leq x \leq 0.9$, see Fig. 5. Another, even more obvious problem is the occurrence of two clear maxima in $S(T)$ for the sample with $x = 0.95$. That is, we observe a thermopower as typical for a Kondo system in a sample, which should be IV regarding the experimental valence of 3.16 ± 0.01 [5,7] and the fact that $T_K \approx T_{\text{CEF}}$. We attribute these observations to the fact that Ce atoms with different environment experience different local Kondo scales T_K^{loc} from below 2 K to above 50 K as suggested previously based on specific heat and susceptibility measurements [7,10]. In fact, as will be demonstrated below, the local Kondo temperature of Ce sites without Pd nearby neighbor may reach even much larger values as in intermediate valent CeRh. Due to this site dependence of the Kondo scale the configuration-crossover model applied to CeRh cannot be used for an analysis of the thermopower of the substituted samples.

Instead we will analyze in the following the thermopower for $x = 0.95$, i.e., the substituted sample with the lowest amount of Pd/Rh disorder, by separating it into contributions from Ce ions with different environment using the Gorter-Nordheim relation Eq. (2). In the CrB structure type Ce is surrounded by seven transition metal atoms in the first coordination sphere at distances of 2.88–3.17 Å. For a Pd content of 5% we then find that 70% of the Ce ions have only Rh nearby neighbors, while 26% have one Pd as neighbor and the remaining 4% more than one Pd neighbor. Assuming that the Ce ions with only Rh nearby neighbors experience the same Kondo scale as the ones in CeRh we may describe the magnetic contribution to the thermopower $S_{\text{mag}} \rho_{\text{mag}}$ of the sample with $x = 0.95$ as a sum of an IV contribution ($S_{\text{IV}} \rho_{\text{IV}}$) from those Ce ions and a Kondo contribution ($S_K \rho_K$) from the other ones. Using Eq. (2) we obtain for the thermopower of

$x = 0.95, S_{0.95}$:

$$S_{0.95}\rho_{0.95} = 0.7S_{IV}\rho_{IV} + 0.3S_K\rho_K + S_{ref}\rho_{ref}, \quad (4)$$

where $S_{IV}\rho_{IV} = S_{1.0}\rho_{1.0} - S_{ref}\rho_{ref}$. ρ_{IV} , and ρ_K refer to the corresponding contributions to the electrical resistivities and are calculated from $\rho_{1.0} = \rho_{IV} + \rho_{ref}$ and $\rho_{0.95} = 0.7\rho_{IV} + 0.3\rho_K + \rho_{ref}$. The Kondo contribution S_K obtained from such a calculation is shown in the main plot of Fig. 4. A shoulder appears around 80 K, exactly at the position of the high- T maximum in $S(T)$ of the samples with $x \leq 0.8$ as indicated by the vertical line. For comparison we also show the thermopower curve for $x = 0.8$. We would like to stress that neither S nor ρ of the samples with $x = 0.95$ and $x = 1$ have a corresponding feature. Thus, it appears that the thermopower of CePd_{0.95}Rh_{0.05} contains contributions from different Ce sites: Those with no Pd neighbors are in the IV state and behave roughly as the ones in CeRh with $T_K^{loc} > 300$ K. The others with at least one Pd neighbor experience an (average) Kondo scale of about 20 K. It is responsible for the low- T maximum in the thermopower of this sample and—in combination with CEF splitting—for the shoulder visible in S_K at 80 K.

The fact that the separation into S_K and S_{IV} works is rather surprising since the validity of Eq. (2) may be questioned for our system. It is based on the Sommerfeld approximation and assumes independent scattering processes and a validity of the Wiedemann-Franz law. Therefore, it is probably not a good approximation for dense Kondo systems [35]. However, it works at least qualitatively in our case. In view of the simplicity of the model it is not surprising that the maximum around 200 K is still seen in S_K . In addition several other points may also play a role: Our calculation is very sensitive to uncertainties of the geometry factors for the resistivities. Moreover, CeRh is probably not an ideal reference. In particular, the Kondo scale of the IV sites may be lower in the substituted sample. Our calculation is therefore only a very rough estimate for S_K . Finally, we only look at the nearby neighbors and ignore those at larger distance. In fact, we suspect, that even the Ce ions with only one nearby Pd neighbor see a variation of T_K^{loc} due to the details in their farther environment. However, this variation is not sufficiently strong to mask two clearly separated features. This situation is different for the samples with lower x . The increasing amount of Pd leads to many different local Ce environments. The resulting disorder gives rise to a broad distribution of T_K and a smearing of the maximum in $S(T)$. Moreover, CeRh is most probably no longer a good reference for those Ce ions, which still have only Rh nearby neighbors, e.g., due to the increasing lattice constant. This makes a separation similar to the one done for $x = 0.95$ impossible.

IV. DISCUSSION

A. Power-law behavior of S/T

We first discuss the large values of $S(T)$ at low T . Figure 5 shows S/T vs T in a doubly logarithmic representation. Close to the critical concentration $x_c = 0.87$ we find roughly a power-law dependence $S/T \propto T^{-\lambda}$ with $\lambda = 0.72$ below 30 K. The exponent is almost constant for the concentration range $0.7 \leq x \leq 0.87$ as seen from the similar slope of the corresponding curves (upper inset). At a higher Rh concentration of $x = 0.9$ the S/T curve bends down towards

low T . A power law with smaller λ can describe the data only below 10 K. On the other side, the $x = 0.6$ curve has a kink at the ferromagnetic transition with an almost constant S/T below T_C . The concentration dependence of λ is shown in the lower inset of Fig. 5 illustrating the small variation of λ for $0.7 \leq x \leq 0.87$.

The observed power laws of S/T vs T for CePd_{1-x}Rh_x differ from the logarithmic divergence found at the antiferromagnetic QCPs in YbRh₂Si₂ [36] and CeCu_{6-x}Au₆ [37,38] and close to a QCP of so far unknown nature in YbAgGe [39,40]. In fact, power-law dependencies of S/T are rarely reported. An exception is U_{0.05}Y_{0.95}Al₂ with $S/T \propto T^{-0.5}$ probably caused by a two-channel Kondo effect [41]. However, since a negative thermopower is predicted for Ce systems in such a case [42], we may rule out a two-channel Kondo effect for CePd_{1-x}Rh_x.

The observed behavior of S/T in CePd_{1-x}Rh_x therefore appears rather unique. Power-law dependencies with similar exponents have been found below about 5 K for several other quantities, e.g., the specific heat divided by temperature, the ac susceptibility, and the μ SR spin-relaxation rate [8,10,11,43]. They have been attributed to the possible formation of a quantum Griffith's phase in the substitution range of $0.8 \leq x \leq 0.9$. However, our $S(T)$ data end at comparably high temperatures of about 2 K, i.e., practically above the respective T range. Therefore it would be somewhat speculative to interpret our data within this scenario, in particular, because there is no theoretical prediction for the transport properties of a ferromagnetic quantum Griffith's phase [44]. Instead, we will restrict ourselves to a qualitative discussion. For a Ce-based Kondo system with a Fermi-liquid ground state $S(T)$ is expected to have a large maximum around T_K [15–17], while S/T should saturate to a constant value of the order of $\gamma/N_A|e| \propto 1/T_K$ at very low T [45,46]. Here, N_A is Avogadro's constant and e is the electron charge. The observation of enhanced thermopower values without a clear low-temperature maximum is therefore in line with a broad distribution of local Kondo temperatures, while the strongly increasing S/T and the absence of saturation can be attributed to the presence of Ce sites with a very low T_K^{loc} that remain unscreened at least down to 2 K. A similar effect, namely a strong enhancement of S over an extended T range due to disorder around the hybridizing $4f$ ion has been observed in YbNi₂B₂C [47]: Unannealed samples of this material have a small number of Yb sites of the order of 1% with a disordered environment that leads to a distribution of Kondo temperatures for these sites. As a result the thermopower of unannealed samples is strongly enhanced compared to annealed ones.

B. Role of disorder

It is rather unexpected that the disorder introduced by substitution in CePd_{1-x}Rh_x appears to be of minor importance for $x \leq 0.6$, while it is highly relevant at larger Rh content and even up to $x = 0.95$. We suspect, that the crucial number in CeRh_{1-x}Pd_x is the amount of Ce sites without Pd nearby neighbor. The corresponding fraction c_{IV} is plotted in the inset to Fig. 6. Our thermopower analysis suggests that these sites are in an IV state, while the others experience low local Kondo scales, which is corroborated by the substitution dependence

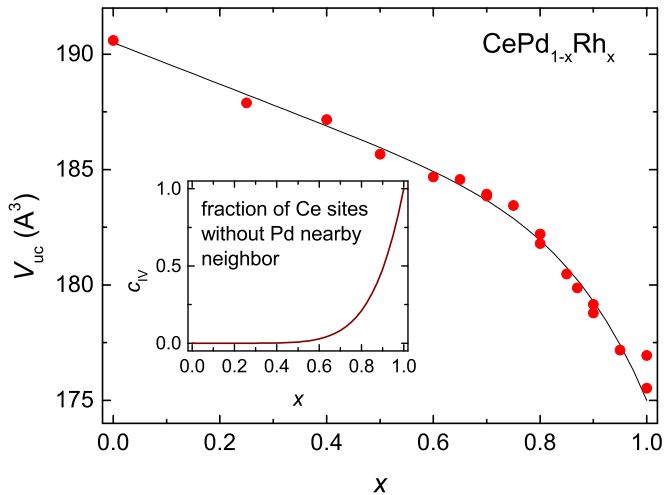


FIG. 6. (Color online) Main plot: Unit cell volume vs x taken from Ref. [7]. The line is a fit consisting of a linear contribution and one proportional to the amount of Ce ions without Pd nearby neighbors: $A_1x + A_2c_{IV}$. Inset: Fraction of Ce ions with a Pd-free environment.

of the unit-cell volume. It can be described almost perfectly by a sum of two contributions, one proportional to x and one proportional to c_{IV} , cf. main plot of Fig. 6. Thus, the deviation from Vegard's law around $x = 0.7$ can be simply explained by an increasing number of IV Ce sites with a Pd-free environment. From the inset to Fig. 6 we see that c_{IV} is below 5% up to $x = 0.65$ and increases rapidly for larger x . This is exactly the concentration range, for which disorder strongly influences the properties of the system as visible, e.g., from the smearing of the ferromagnetic transition in specific heat and the broad distribution of local T_K^{loc} .

This idea is also in line with pressure experiments on a single crystal with $x = 0.4$ [48]. The thermopower measured at ambient pressure looks very similar to our data with negative values at low T , a rather sharp maximum close to T_C and a second, broad maximum around 100 K. As the pressure is increased up to 6.6 GPa, the low- T maximum changes to a shoulder, while the high- T maximum shifts only moderately to about 150 K. At $p > 6.6$ GPa, the authors find a sudden change of the thermopower curves to an IV-like shape with a (suspected) single maximum above room temperature. That is, the system changes as a whole from a ferromagnetic Kondo lattice to the IV state, despite the presence of significant Pd/Rh disorder. This is in contrast to the behavior upon substitution, where we find no low- T maximum or shoulder over an extended x range. Instead we have clear evidence for the presence of Ce sites with different behavior and the simultaneous occurrence of Kondo-like and IV contributions to the thermopower for $x = 0.95$, a system with much lower atomic disorder than $x = 0.4$ but a significant percentage of Ce sites without Pd neighbor.

The overall behavior we observe in $\text{CePd}_{1-x}\text{Rh}_x$, namely a local Kondo scale strongly depending on the respective

numbers of Rh and Pd nearest neighbors, is in line with established knowledge on parameters governing hybridization in unstable $4f$ systems. According to both experimental results and theoretical considerations, this hybridization presents a broad maximum at half filling of the valence shell of the ligands and decreases significantly when this shell is emptied or filled [49,50]. Furthermore it increases from s - to p - and to d -ligand shells. Accordingly, hybridization in binary Ce-Rh and ternary Ce-Rh- X compounds (X : p element), with one hole in the $4d$ Rh shell, is always significantly larger than in homologous compounds, binary Ce-Pd and Ce-Pd- X , where the $4d$ Pd states are almost completely filled [49,51]. Thus it is not surprising that in $\text{CeRh}_{1-x}\text{Pd}_x$ the local T_K is strongly decreasing with the ratio between the number of nearest Rh and Pd neighbors. The surprising result is the huge decrease of T_K when replacing just one Rh by Pd [from above 300 K for CeRh to about 20 K as suggested by the shoulder in $S(T)$ for $x = 0.95$], while substituting further Rh by Pd seemingly has a much weaker effect. A possible explanation is the strong dependence of T_K on the orbital degeneracy. In pure CeRh, T_K is of the order of the CEF splitting. Thus, the whole $J = 5/2$ multiplet with a degeneracy $N = 6$ is involved in the formation of the Kondo singlet. Substituting one Rh by Pd results in T_K dropping significantly below the overall CEF splitting. Thus only the lowest two CEF doublets, or may be even only the ground-state CEF doublet gets involved in the formation of the Kondo singlet. The resulting decrease of the effective orbital degeneracy to $N = 2$ strongly enhances the drop of T_K . Since N cannot drop further, this effect is not anymore relevant for further decreasing T_K .

V. SUMMARY

In summary, we obtain the following overall picture for $\text{CePd}_{1-x}\text{Rh}_x$ from the analysis of the thermopower: At low Rh content, the system is a ferromagnetic Kondo system with a Curie temperature of about 6 K, a small Kondo scale with $T_K \leq T_C$ and an overall CEF splitting of 210 K. As the Rh content increases above $x = 0.6$ the presence of different Ce environments leads to a broad distribution of local Kondo scales from very small values to above 50 K. This gives rise to large thermopowers over an extended temperature range and increasing values of S/T down to 2 K. Close to the critical concentration $S(T)$ vs T assumes a power-law dependence down to 2 K, a behavior rarely observed in thermopower measurements before. For high Rh content, those Ce ions with a Pd-free environment are in the IV state, while the others still experience a comparable low Kondo scale in combination with CEF splitting. Finally, pure CeRh is an IV compound.

ACKNOWLEDGMENT

The authors acknowledge financial support from COST P-16 action (Belgium).

[1] A. J. Schofield, *Phys. Status Solidi B* **247**, 563 (2010).

[2] F. Steglich, *Philos. Mag.* **94**, 3259 (2014).

[3] M. Brando, D. Belitz, F. M. Grosche, and T. R. Kirkpatrick, [arXiv:1502.02898](https://arxiv.org/abs/1502.02898).

- [4] J. P. Kappler, M. J. Besnus, A. Herr, A. Meyer, and J. G. Sereni, *Physica B* **171**, 346 (1991).
- [5] J. G. Sereni, E. Beaurepaire, and J. P. Kappler, *Phys. Rev. B* **48**, 3747 (1993).
- [6] J. G. Sereni, R. KÜchler, and C. Geibel, *Physica B* **359–361**, 41 (2005).
- [7] J. G. Sereni, T. Westerkamp, R. KÜchler, N. Caroca-Canales, P. Gegenwart, and C. Geibel, *Phys. Rev. B* **75**, 024432 (2007).
- [8] T. Westerkamp, M. Deppe, R. KÜchler, M. Brando, C. Geibel, P. Gegenwart, A. P. Pikul, and F. Steglich, *Phys. Rev. Lett.* **102**, 206404 (2009).
- [9] S. Hartmann, M. Deppe, N. Oeschler, N. Caroca-Canales, J. Sereni, and C. Geibel, *J. Optoelectron. Adv. Mater.* **10**, 1607 (2008).
- [10] A. P. Pikul, N. Caroca-Canales, M. Deppe, P. Gegenwart, J. G. Sereni, C. Geibel, and F. Steglich, *J. Phys. Condens. Matter* **18**, L535 (2006).
- [11] D. T. Adroja, A. D. Hillier, J.-G. Park, W. Kockelmann, K. A. McEwen, B. D. Rainford, K.-H. Jang, C. Geibel, and T. Takabatake, *Phys. Rev. B* **78**, 014412 (2008).
- [12] D. Jaccard and J. Siero, in *Valence Instabilities*, edited by P. Wachter and H. Boppart (North-Holland, Amsterdam, 1982).
- [13] J. H. Moeser, F. Steglich, and G. von Minnigerode, *J. Low Temp. Phys.* **15**, 91 (1974).
- [14] P. Sun and F. Steglich, *Phys. Rev. Lett.* **110**, 216408 (2013).
- [15] V. ZlatiĆ and R. Monnier, *Phys. Rev. B* **71**, 165109 (2005).
- [16] N. E. Bickers, D. L. Cox, and J. W. Wilkins, *Phys. Rev. B* **36**, 2036 (1987).
- [17] G. D. Mahan, *Phys. Rev. B* **56**, 11833 (1997).
- [18] R. Cibin, D. Jaccard, and J. Sierro, *J. Magn. Magn. Mater.* **108**, 107 (1992).
- [19] Y. Bando, J. Sakurai, and E. V. Sampathkumaran, *Physica B* **186–188**, 525 (1993).
- [20] M. Oĉko, D. Drobac, B. Buschinger, C. Geibel, and F. Steglich, *Phys. Rev. B* **64**, 195106 (2001).
- [21] S. Paschen, B. Wand, G. Sparr, F. Steglich, Y. Echizen, and T. Takabatake, *Phys. Rev. B* **62**, 14912 (2000).
- [22] M. Deppe, P. Pedrazzini, N. Caroca-Canales, C. Geibel, and J. G. Sereni, *Physica B* **378–380**, 96 (2006).
- [23] L. L. Hirst, *Phys. Rev. B* **15**, 1 (1977).
- [24] U. Gottwick, K. Gloos, S. Horn, F. Steglich, and N. Grewe, *J. Magn. Magn. Mater.* **47–48**, 536 (1985).
- [25] R. Gumeniuk, R. Sarkar, C. Geibel, W. Schnelle, C. Paulmann, M. Baenitz, A. A. Tsirlin, V. Guritanu, J. Sichelschmidt, Yu. Grin, and A. Leithe-Jasper, *Phys. Rev. B* **86**, 235138 (2012).
- [26] M. S. Torikachvili, B. K. Davis, K. Kothapalli, H. Nakotte, A. J. Schultz, E. D. Mun, and S. L. Bud'ko, *Phys. Rev. B* **84**, 205114 (2011).
- [27] A. Prasad, V. K. Anand, U. B. Paramanik, Z. Hossain, R. Sarkar, N. Oeschler, M. Baenitz, and C. Geibel, *Phys. Rev. B* **86**, 014414 (2012).
- [28] M. Matusiak, A. Lipatov, A. Gribanov, and D. Kaczorowski, *J. Phys. Condens. Matter* **25**, 265601 (2013).
- [29] E. D. Mun, S. L. Bud'ko, and P. C. Canfield, *J. Phys. Condens. Matter* **23**, 476001 (2011).
- [30] C. Krellner, N. S. Kini, E. M. BrÜning, K. Koch, H. Rosner, M. Nicklas, M. Baenitz, and C. Geibel, *Phys. Rev. B* **76**, 104418 (2007).
- [31] A. K. Bhattacharjee and B. Coqblin, *Phys. Rev. B* **13**, 3441 (1976).
- [32] S. Maekawa, S. Kashiba, M. Tachiki, and S. Takahashi, *J. Phys. Soc. Jpn.* **55**, 3194 (1986).
- [33] V. ZlatiĆ, B. HorvatiĆ, I. Milat, B. Coqblin, G. Czycholl, and C. Grenzbach, *Phys. Rev. B* **68**, 104432 (2003).
- [34] U. Köhler, N. Oeschler, F. Steglich, S. Maquilon, and Z. Fisk, *Phys. Rev. B* **77**, 104412 (2008).
- [35] K. H. Fischer, *Z. Phys. B* **76**, 315 (1989).
- [36] S. Hartmann, N. Oeschler, C. Krellner, C. Geibel, S. Paschen, and F. Steglich, *Phys. Rev. Lett.* **104**, 096401 (2010).
- [37] J. Benz, C. Pfleiderer, O. Stockert, and H.v. Löhneysen, *Physica B* **259–261**, 380 (1999).
- [38] I. Paul and G. Kotliar, *Phys. Rev. B* **64**, 184414 (2001).
- [39] E. D. Mun, S. L. Bud'ko, and P. C. Canfield, *Phys. Rev. B* **82**, 174403 (2010).
- [40] G. M. Schmiedeshoff, E. D. Mun, A. W. Lounsbury, S. J. Tracy, E. C. Palm, S. T. Hannahs, J.-H. Park, T. P. Murphy, S. L. Bud'ko, and P. C. Canfield, *Phys. Rev. B* **83**, 180408(R) (2011).
- [41] V. H. Tran, *Acta Phys. Pol. A* **113**, 387 (2008).
- [42] T.-S. Kim and D. L. Cox, *Phys. Rev. Lett.* **75**, 1622 (1995).
- [43] M. Brando, T. Westerkamp, M. Deppe, P. Gegenwart, C. Geibel, and F. Steglich, *J. Phys. Conf. Ser.* **200**, 012016 (2010).
- [44] D. Nozadze and T. Vojta, *Eur. Phys. Lett.* **95**, 57010 (2011).
- [45] K. Behnia, D. Jaccard, and J. Flouquet, *J. Phys. Condens. Matter* **16**, 5187 (2004).
- [46] H.-U. Desgranges and K. D. Schotte, *Phys. Lett. A* **91**, 240 (1982).
- [47] M. A. Avila, S. L. Bud'ko, and P. C. Canfield, *Phys. Rev. B* **66**, 132504 (2002).
- [48] P. Pedrazzini, D. Jaccard, M. Deppe, C. Geibel, and J. G. Sereni, *Physica B* **404**, 2898 (2009).
- [49] A. Iandelli and A. Pallenzone, *Handbook on the Physics and Chemistry of Rare Earths, Vol. 2*, edited by K. A. Gschneider, Jr. and L. Eyring (North-Holland, Amsterdam, 1979).
- [50] D. D. Koelling, B. D. Dunlap, and G. W. Crabtree, *Phys. Rev. B* **31**, 4966 (1985).
- [51] V. Sechovský and L. Havela, *J. Alloys Compd.* **225**, 444 (1995).